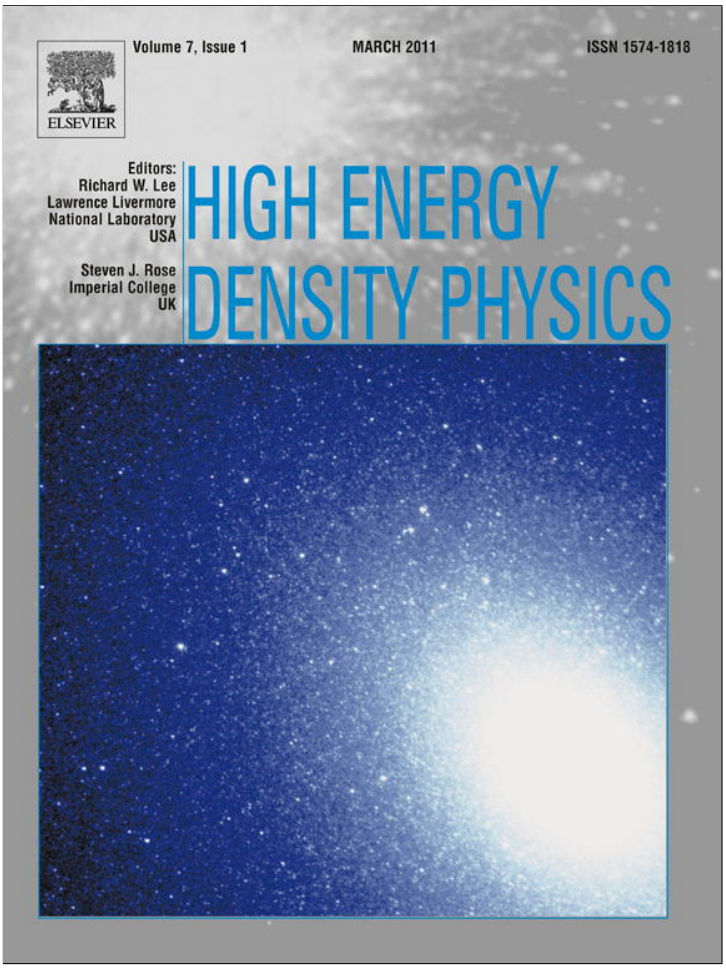

(This is a sample cover image for this issue. The actual cover is not yet available at this time.)

High Energy Density Physics 7 (2011) 105–109

Contents lists available at ScienceDirect

High Energy Density Physics

journal homepage: www.elsevier.com/locate/hedp

Short Communication

Precision X-ray spectroscopy of intense laser-plasma interactions

N.C. Woolsey [a,*], R.J. Clarke [b], D. Doria [c], L.A. Gizzi [d], G. Gregori [e], P. Hakel [f], S.B. Hansen [g], P. Koester [d], L. Labate [d], T. Levato [d], B. Li [b], M. Makita [c], R.C. Mancini [f], J. Pasley [a,b], P.P. Rajeev [b], A.P.L. Robinson [b], E. Wagenaars [a], J.N. Waugh [a], N. Booth [a,b]

[a] Department of Physics, University of York, Heslington, York YO10 5DD, UK
[b] Central Laser Facility, STFC Rutherford Appleton Laboratory, Didcot OX11 0QN, UK
[c] Department of Physics and Mathematics, The Queen's University of Belfast, Belfast BT1 4NN, UK
[d] ILIL, Istituto Nazionale di Ottica, UOS "Adriano Gozzini", CNR, Via G. Moruzzi 1, Pisa, Italy
[e] Department of Physics, University of Oxford, OX4 1PJ, UK
[f] Department of Physics, University of Nevada, Reno, NV 89557-0208, USA
[g] Sandia National Laboratories, Albuquerque, NM 87185, USA

ARTICLE INFO

Article history:
Received 2 March 2011
Accepted 2 March 2011
Available online 17 March 2011

Keywords:
X-ray polarisation spectroscopy
Fast ignition
Petawatt laser – matter interactions

ABSTRACT

Polarisation sensitive emission spectroscopy measurements are reported for a petawatt laser-solid target interaction at intensities up to 5×10^{20} W cm^{-2}. These measurements were single-shot and used pairs of highly-orientated graphite spectrometers to resolve the sulphur Ly-α doublet. The sulphur Ly-α_1 component shows a large positive polarisation indicative of a low energy electron beam in the plasma, the Ly-α_2 component acts as a cross-spectrometer calibration. The measurements show a significant anisotropic or beam-like component to a cold return current.

1. Introduction

The fast ignition approach to inertial confinement fusion uses a particle beam to ignite a highly compressed target of deuterium and tritium by rapidly heating a small region of the target to thermonuclear temperatures. In the most widely considered scheme an ultra-intense laser generates a relativistic electron beam that propagates through an extended dense plasma to the highly compressed deuterium – tritium fuel [1]. The many advantages of fast ignition, which include a reduction in the energy required to compress the target, a relaxation of target symmetry and higher gains, has stimulated much interest in this approach. Establishing electron fast ignition as a viable scenario demands addressing uncertainties in electron currents, electron distributions and beam divergence. This article focuses on the X-ray polarisation spectroscopy method [2] to infer beam-like properties of the electron transport in a solid target.

Most experimental studies of electron beam fast ignition focus on the interaction of an ultra-intense laser with an over-critical density ablation plasma created at the surface of a solid density target [3]. Our understanding of the interaction physics is often inferred from angular and spectral distributions of particles (electrons, protons and heavier ions) leaving the target, X-ray K-α imaging [4] and spectroscopy [5,6]. These observations suggest that laser-solid target interactions are interesting secondary sources of temporarily short and synchronised X-rays [7] and particles [8].

In this article we demonstrate how to infer spectral line polarisation from petawatt scale laser-plasma experiment in a single-shot and how such measurements provide unique and valuable information about the electron distributions in these targets.

2. Fast electron transport

The interaction between the fast electron beam and target is predominantly collision-free; to sustain the intense fast electron current a cooler, thus more collisional, population of electrons counter-stream to form a return current. This return current is the main source of target heating [9–12] and can result in target temperatures of several hundred eV that is sufficient to strip elements up to nickel ($Z = 28$) to H-like and/or He-like ionisation states [13]. An isotropic velocity distribution, which is typical of a return current, will lead to statistical population of magnetic sublevels of an excited state. This results in emission lines with no net polarisation. In comparison the presence of a beam-like

* Corresponding author.
E-mail address: nigel.woolsey@york.ac.uk (N.C. Woolsey).

1574-1818/$ – see front matter © 2011 Elsevier Ltd. All rights reserved.
doi:10.1016/j.hedp.2011.03.001

component can result in a polarisation of emission lines. This polarisation results from a preferential population of certain magnetic sublevels [14–16]. A beam-like component to the fast electrons is well established [17]. This paper highlights results that show a beam-like component to the return current.

3. Polarisation emission spectroscopy

Beam-like components to fast electron populations are typical of ultra-intense laser-plasma and laser-solid interactions [18]. Competition between excitation due to the strongly anisotropic fast electrons and the predominately isotropic and collisional return current ultimately determines the degree of polarisation.

An appropriate choice of emission line, laser and target combination, and spectrometer geometry enables a measurement of current anisotropy. In an ultra-intense laser-plasma and laser-solid experiment, fast electrons generated at the laser-interaction region stream through the target establishing an electrostatic field. This electrostatic field defines a quantisation direction to which collisionally excited states are aligned. This can result in preferential population of some magnetic sublevels (determined by quantum number m_J) within an atomic energy level. Here we choose the Ly-α transition of hydrogen-like nickel, which is dipole allowed and has a distinctive σ-polarisation due the $\Delta m_J = \pm 1$ transitions and a π-polarisation due to the $\Delta m_J = 0$ transition. The degree of polarisation in an emission line determines the relative population in a magnetic sublevel and it is possible to relate this to the degree of electron velocity anisotropy. Thus, by measuring the polarisation of a spectral line, a powerful method of examining this anisotropy, which is a key feature of the non-thermal aspect of a laser-produced plasma, exists.

To measure spectral line polarisation we exploit a property of classical x-ray scattering combined with Bragg diffraction. The intensity of a π-polarised electromagnetic wave (I_π) scattering from an electron depends on the scattering angle φ as cos [2](φ). At $\varphi = 90^\circ$ the intensity falls to zero whilst the intensity of σ-polarisation (I_σ) remains constant at all angles. The degree of polarisation P is calculated from

$$P = (I_\pi - I_\sigma)/(I_\pi + I_\sigma) \quad (1)$$

When combined with Bragg diffraction it is necessary that the Bragg angle $\theta_B = \varphi/2 = 45^\circ$. To extract both I_σ and I_π it is necessary to rotate the spectrometer 90° or use two spectrometers in an orthogonal geometry. Keiffer et al. [15] first applied this method to laser plasmas and the Al He-α transition using an ammonium dihydrogen phosphate (ADP) crystal at a Bragg angle of 45°, to compare orthogonal polarisations, i.e., I_σ and I_π. The application of polarisation emission spectroscopy has required the development of sophisticated spectroscopic models [19,20] to relate the observed polarisation characteristics to anisotropic features in the plasma. Recently Inubushi and co-workers [21] have used chlorine doped buried layers and polarisation spectroscopy to study the angular spread of electron velocity distribution in solid targets.

At the high-energy densities typical of an ultra-intense laser-solid interaction the Ly-α and He-α transitions of medium Z elements are often bright emitters of radiation. The Ly-α transition consists of two spin-orbit split components the Ly-α_2 ($1s\ ^2S_{1/2}$–$2p\ ^2P_{1/2}$) and the Ly-α_1 ($1s\ ^2S_{1/2}$–$2p\ ^2P_{3/2}$). These components consist of, respectively, 4 and 6 magnetic-sublevel-to-magnetic-sublevel transitions. FAC (flexible atomic code [22]) calculations in Fig. 1 show the polarisation P of the sulphur ($Z = 16$) Ly-α components as a function of beam energy. The figure illustrates that the Ly-α_1 transition polarisation varies, from a large positive value when beam energy to transition energy ratio, $\epsilon_{beam}/\Delta\varepsilon$, is approximately 1,

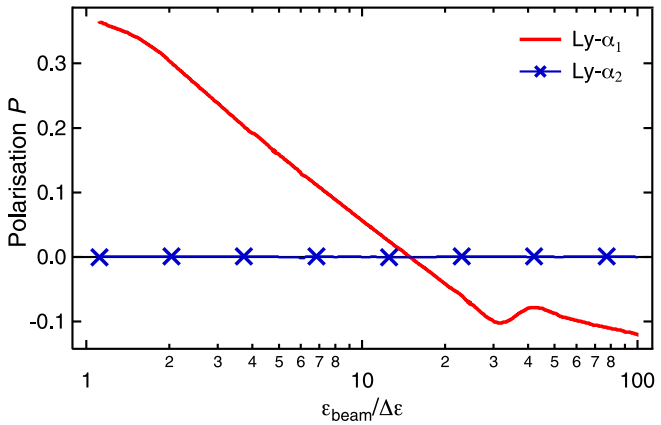

Fig. 1. Spectral line polarisation, P, calculations for the sulphur Ly-α doublet as a function of the ratio of beam impact electron energy to excitation potential energy ($\epsilon_{beam}/\Delta\varepsilon$). The Ly-$\alpha_1$ component (solid line) shows strong polarisation, whilst the Ly-α_2 (crosses) component is unpolarised. The calculations assume collisional excitation by the fast electron beam.

to no polarisation at $\epsilon_{beam}/\Delta\varepsilon \sim 15$, and a negative polarisation for larger ratios. From a semi-classical view this occurs because at low energy an incident electron beam causes an excitation with an electron oscillating along the beam axis. The consequence is that the magnetic-sublevel-to-magnetic-sublevel cross-sections result in emission that is π-polarised, resulting in a positive P. This changes as the incident electron beam energy increases and excitation results from a pulsed electric field. For a pulsed field the excited electron oscillates in a plane perpendicular to the beam, populating magnetic-sublevel-to-magnetic-sublevels that result in σ-polarised radiation and a negative P. The sign of a polarisation measurement immediately indicates the energy of the exciting electron beam. In comparison, the Ly-α_2 transition remains unpolarised at all beam energies. This component is therefore used as a cross calibration for the Ly-α_1.

The need for single-shot measurement restricts the spectrometer choice to crystals with high reflectivity. A highly-orientated graphite (HOPG) crystal is ideal and when orientated with (002) planes with a $2d = 6.708$ Å at $\theta_B = 45^\circ$ suits sulphur Ly-α in 1st order and nickel ($Z = 28$) Ly-α in 3rd order. The sulphur Ly-α components (Ly-α_2 at 2619.6 eV and Ly-α_1 at 2622.6 eV) diffract at 44.87° and 44.81° respectively. Rocking curve calculations, shown in Fig. 2, for the HOPG (002) crystal at the sulphur Ly-α energies demonstrates that photons falling on the crystal with the electric

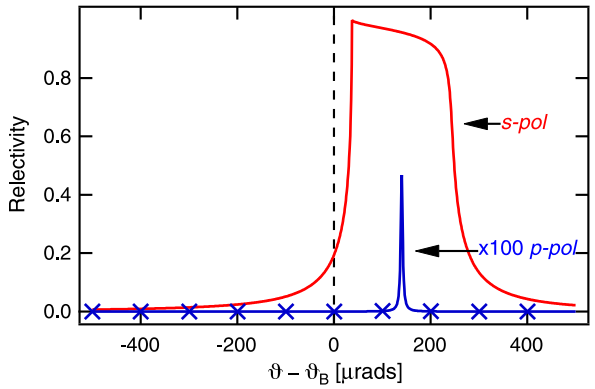

Fig. 2. Rocking curve calculations for s- (solid line) and p- (crosses) polarised radiation diffracting from the (002) orientation of a perfect highly-orientated graphite (HOPG) crystal.

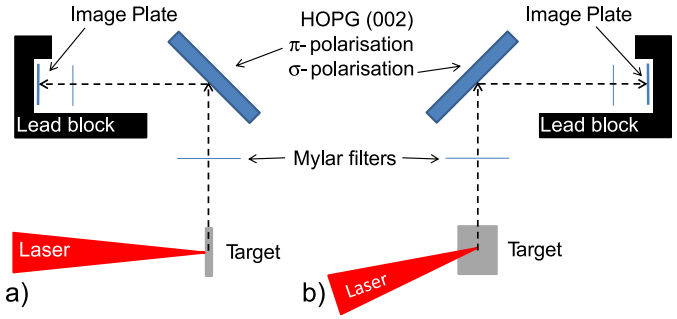

Fig. 3. This schematic shows the layout of the "top" spectrometer pair. a) Shows the target side-on and the spectrometer configuration for measuring π-polarised (with respect to the target surface normal, the quantisation axis) X-ray emission, and b) shows the target face on and the spectrometer configuration for σ-polarised emission. The HOPG crystals are orthogonal and set at 45° to the target surface normal. Extensive lead shielding is necessary to limit background exposure of the image plate detectors.

field in the plane of incidence (*p*-polarised) are not diffracted. The *s*- and *p*- integrated reflectivity differs by 5-orders-of-magnitude. For single-shot measurements it is necessary to use two identical spectrometers and record both polarisations simultaneously.

4. Experimental configuration

The Target Area Petawatt (TAP) of the Vulcan laser facility was used for this experiment. The Vulcan laser, based at the Rutherford Appleton Laboratory, UK, is a chirped pulse amplified Nd:Glass laser operating at a wavelength of 1054 nm. The laser repetition rate is approximately 1 shot per hour. In this experiment the TAP beam delivered 300 J in a 1 ps duration laser pulse with a peak to amplified spontaneous emission contrast at a nanosecond of 10^7 and at approximately 10 ps of 10^6. The p-polarised laser beam was focused onto mass-limited [23] targets with an f/3 off-axis parabolic mirror at an angle of incidence of 40°. At best focus the spot diameter of 5 μm contained 70% of the energy and by moving the target through focus the laser intensity was varied between 5×10^{20} and 10^{19} W/cm^2.

The targets were mass-limited to ensure the creation of hot-dense plasmas, and consisted of 100 μm square slabs of either 25 μm thick polysulphone ($C_{27}H_{26}O_6S$) or 10 μm nickel mounted from 10 μm diameter copper wires. Polysulphone is a thermoplastic polymer of density 1.24 g/cm^3 with excellent mechanical and thermal stability and is ideal for targets. The primary diagnostic for this experiment was a pair of HOPG (002) crystal spectrometers. The crystals were identical and flat 50 mm by 25 mm, 2 mm thick ZYA graphite with a mosaic spread of 0.4 ± 0.1°.

The quantisation axis is in the direction of the target normal, the line of sight of each crystal spectrometer is perpendicular to this axis. The crystals were positioned 200 mm above the target, see Fig. 3. In each pair, the crystals are set orthogonal to one another and perpendicular to the quantisation axis. Each crystal diffracts with a Bragg angle of 45°, thus one crystal diffracts only σ-polarised radiation whilst the other crystal diffracts only π-polarised radiation. The spectra are recorded on image plates placed 200 mm from the crystals. The crystals were protected from target debris with 6 μm thick mylar film and the image plates were made light tight with 25 or 50 μm thick beryllium windows. Considerable attention was paid to shielding the spectrometers with lead bricks to limit background. Data were extracted from the image plates using Fujifilm BAS2500 scanner following established procedures [24].

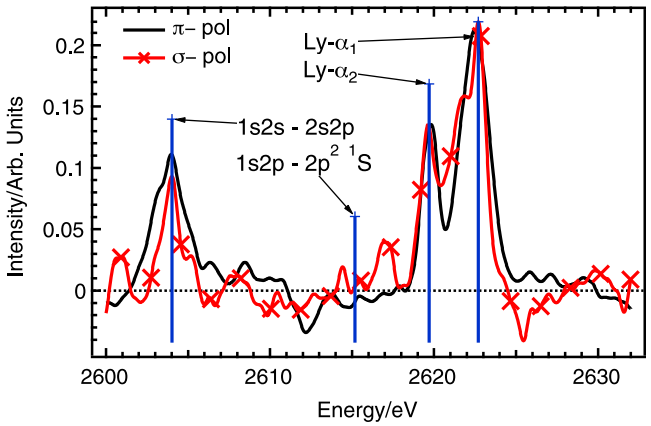

Fig. 5. Traces along the spectral direction of the corrected spectrometer data of the σ- (crosses) and π- (solid line) polarised sulphur Ly-α transition taken from data similar to Fig. 4. The spectra are compared to spectral line positions (vertical lines) taken from NIST Atomic Spectra Database [25].

4.1. Sulphur Ly-α_1

A set of results from the top HOPG spectrometers is shown in Fig. 4. The data is of the sulphur Ly-α transition taken from a polysuphane target when shot at 10^{19} W/cm^2. The upper image is from the crystal orientated to diffract radiation with π-polarised (electric field perpendicular to quantisation axis) radiation and the lower image shows the σ-polarised component. In both cases the Ly-α doublet is resolved. There is a difference in the background fogging due to the relative orientation of the spectrometers, see Fig. 3. This background is accounted for in the data analysis and uncertainties associated with background corrections contribute to the quoted errors.

The spectra corrected for background are shown in Fig. 5. To enable comparison between the spectrum taken from each crystal, noting that the integrated reflectivities of the crystals in each pair are identical, the integrated line intensities of the unpolarised Ly-α_2 are matched. A Voigt fitting procedure is used to fit the Ly-α doublet and determine the integrated intensity of the Ly-α_1 line. The integrated intensity of the Ly-α_1 for σ- ($I\sigma_\sigma$) and π- (I_π) polarisation is

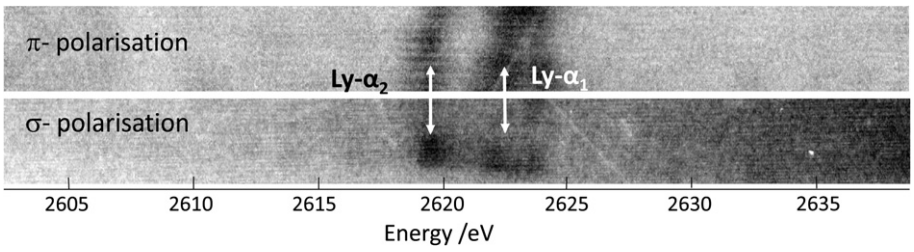

Fig. 4. Example raw data showing sulphur Ly-α spectra recorded using the "top" spectrometer pair. Note that the Ly-α doublet is clearly resolved. See Fig. 3 for the definition of π- and σ- polarisation.

then input into Eq. (1) to determine the degree of polarisation. The uncertainties due to background subtraction and minor positioning differences between the crystals in each pair are included in the errors.

The degree of polarisation inferred from the analysis of the sulphur Ly-α_1 in Fig. 5 is $P = +0.22 \pm 0.04$. This is a positive and large polarisation. The net polarisation of the Ly-α_1 line results from a competing balance between collisional excitation from anisotropic populations of electrons which result in a polarisation and isotropic populations of electrons which depolarise the emission. The large polarisation suggests that excitation due to depolarising isotropic electron populations is small and an anisotropic population dominates. Furthermore, as the polarisation is positive and large the anisotropic population must be relatively cool. A simple comparison with Fig. 1 suggests that for $P \sim +0.2$ the beam energy, ε_{beam}, is 4 times the excitation energy, $\Delta\varepsilon$, giving a beam energy of order 10 keV. This is a temperature two-orders-of-magnitude lower than the MeV temperatures anticipated for the fast electron beam. This suggests a beam-like component associated with the return current, which is responsible for exciting the Ly-α transition, and that the return current in an ultra-intense laser interaction can no longer be considered as isotropic.

5. Conclusions

Polarisation emission spectroscopy of mid-Z elements has been employed to study the electron velocity anisotropy associated with ultra-intense laser interactions. The intensities of approximately 10^{20} W/cm^2 produce mega-electron volt electron beams, these energies are relevant to fast ignition and the production of secondary sources. By using HOPG spectrometer pairs we have been able to extract single-shot measurements that show large and positive polarisations for the sulphur Ly-α_1 transition. The Ly-α_2 component remains unpolarised and enables accurate determination of the Ly-α_1 polarisation.

The large polarisation indicates that depolarisation of the Ly-α_1 transition due to an isotropic return current is small. The large positive polarisation indicates that the isotropic component of the return current does not excite Ly-α transition which has an excitation potential of 2.6 keV. This suggests that the temperature of the isotropic component is low and possibly around 200 eV. This is broadly in agreement with previous measurement and simulation [26,27]. The excitation of the Ly-α transition leading to a polarisation of $P \sim 0.22$ indicates the presence of an anisotropic or beam-like electron population with temperatures higher than that of the isotropic component of the return current and orders-of-magnitude less than the MeV fast electron temperature.

This suggests that return current distributions are more complex than the simple isotropic model often employed and that return current models should consider anisotropic components to the energy and velocity distributions. Furthermore, the interpretation of spectroscopic measurements from fast electron heated plasmas needs to consider kinetic effects due to anisotropic features of the plasma environment as well as the collisional-radiative model to determine the populations of various excited states.

Acknowledgements

We thank the staff at the Central Laser Facility for their help and expertise in providing the laser, target area and target. We acknowledge funding from the Extreme Light Infrastructure Project, the HiPER project, the United Kingdom Engineering and Physical Sciences Research Council and the Science and Technology Facilities Council.

References

[1] M. Tabak, J. Hammer, M.E. Glinsky, W.L. Kruer, S.C. Wilks, J. Woodworth, E.M. Cambell, M.D. Perry, R.J. Mason, Phys. Plasmas 1 (1994) 1624. http://pop.aip.org/resource/1/phpaen/v1/i5/p1626_s1.
[2] T. Fujimoto, S.A. Kazantsev, Plasma Phys. Control. Fusion 39 (1997) 1267. http://iopscience.iop.org/0741-3335/39/9/002.
[3] J.R. Davies, Plasma Phys. Control. Fusion 51 (2009) 014006. http://iopscience.iop.org/0741-3335/51/1/014006/.
[4] R.B. Stephens, R.A. Snavely, Y. Aglitskiy, F. Amiranoff, C. Andersen, D. Batani, S.D. Baton, T. Cowan, R.R. Freeman, T. Hall, S.P. Hatchett, J.M. Hill, M.H. Key, J.A. King, J.A. Koch, M. Koenig, A.J. MacKinnon, K.L. Lancaster, E. Martinolli, P. Norreys, E. Perelli-Cippo, M. Rabec Le Gloahec, C. Rousseaux, J.J. Santos, F. Scianitti, Phys. Rev. E 69 (2004) 066414. http://pre.aps.org/abstract/PRE/v69/i6/e066414.
[5] J.A. Koch, M.H. Key, R.R. Freeman, S.P. Hatchett, R.W. Lee, D. Pennington, R.B. Stephens, M. Tabak, Phys. Rev. E 65 (2001) 016410. http://link.aps.org/doi/10.1103/PhysRevE.65.016410.
[6] U. Zastrau, P. Audebert, V. Bernshtam, E. Brambrink, T. Kämpfer, E. Kroupp, R. Loetzsch, Y. Maron, Yu. Ralchenko, H. Reinholz, G. Röpke, A. Sengebusch, E. Stambulchik, I. Uschmann, L. Weingarten, E. Förster, Phys. Rev. E 81 (2010) 026406. http://pre.aps.org/abstract/PRE/v81/i2/e026406.
[7] H.-S. Park, D.M. Chambers, H.-K. Chung, R.J. Clarke, R. Eagleton, E. Giraldez, T. Goldsack, R. Heathcote, N. Izumi, M.H. Key, Phys. Plasma 13 (2006) 056309. http://link.aip.org/link/PHPAEN/v13/i5/p056309/s1.
[8] M. Borghesi, A.J. Mackinnon, D.H. Campbell, D.G. Hicks, S. Kar, P.K. Patel, D. Price, L. Romagnani, A. Schiavi, O. Willi, Phys. Rev. Lett. 92 (2004) 055003. http://prl.aps.org/abstract/PRL/v92/i5/e055003.
[9] A.P.L. Robinson, A.R. Bell, R.J. Kingham, Plasma Phys. Control. Fusion 48 (2006) 1063.http://iopscience.iop.org/0741-3335/48/8/002/.
[10] Y. Sentoku, K. Mima, P. Kaw, K. Nishikawa, Phys. Rev. Lett. 90 (2003) 155001. http://prl.aps.org/abstract/PRL/v90/i15/e155001.
[11] Y. Inubushi, T. Kai, T. Nakamura, S. Fujioka, H. Nishimura, K. Mima, Phys. Rev. E 75 (2007) 026401. http://pre.aps.org/abstract/PRE/v75/i2/e026401.
[12] M. Nakatsutsumi, J.R. Davies, R. Kodama, J.S. Green, K.L. Lancaster, K.U. Akli, F.N. Beg, S.N. Chen, D. Clark, R.R. Freeman, C.D. Gregory, H. Habara, R. Heathcote, D.S. Hey, K. Highbarger, P. Jaanimagi, M.H. Key, K. Krushelnick, T. Ma, A. MacPhee, A.J. MacKinnon, H. Nakamura, R.B. Stephens, M. Storm, M. Tampo, W. Theobald, L. Van Woerkom, R.L. Weber, M.S. We, N.C. Woolsey, P.A. Norreys, New J. Phys. 10 (2008) 043046. http://iopscience.iop.org/1367-2630/10/4/043046.
[13] K.U. Akli, S.B. Hansen, A.J. Kemp, R.R. Freeman, F.N. Beg, D.C. Clark, S.D. Chen, D. Hey1, S.P. Hatchett, K. Highbarger, E. Giraldez, J.S. Green, G. Gregori, K.L. Lancaster, T. Ma, A.J. MacKinnon, P. Norreys, N. Patel, J. Pasley, C. Shearer, R.B. Stephens, C. Stoeck, M. Storm, W. Theobald, L.D. Van Woerkom, R. Weber, M.H. Key, Phys. Rev. Lett. 100 (2008) 165002. http://prl.aps.org/abstract/PRL/v100/i16/e165002.
[14] H. Nishimura, Y. Inubushi, M. Ochiai, T. Kai, T. Kawamura, S. Fujioka, M. Hashida, S. Simizu, S. Sakabe, R. Kodama, K.A. Tanaka, S. Kato, F. Koike, S. Nakazaki, H. Nagatomo, T. Johzaki, K. Mima, Plasma Phys. Control. Fusion 47 (2005) B823. http://iopscience.iop.org/0741-3335/47/12B/S64/.
[15] J.C. Kieffer, J.P. Matte, H. Pépin, M. Chaker, Y. Beaudoin, T.W. Johnston, C.Y. Chien, S. Coe, G. Mourou, J. Dubau, Phys. Rev. Lett. 68 (1992) 480.http://prl.aps.org/abstract/PRL/v68/i4/p480_1;
ibid, Phys. Rev. E
48 (1993) 4648.http://pre.aps.org/abstract/PRE/v48/i6/p4648_1.
[16] P. Hakel, R.C. Mancini, C. Harris, P. Neill, P. Beiersdorfer, G. Csanak, H.L. Zhang, Phys. Rev. A 76 (2007) 012716. http://pra.aps.org/abstract/PRA/v76/i1/e012716.
[17] M.H. Key, M.D. Cable, T.E. Cowan, K.G. Estabrook, B.A. Hammel, S.P. Hatchett, E.A. Henry, D.E. Hinkel, J.D. Kilkenny, J.A. Koch, W.L. Kruer, A.B. Langdon, B.F. Lasinski, R.W. Lee, B.J. MacGowan, A. MacKinnon, J.D. Moody, M.J. Moran, A.A. Offenberger, D.M. Pennington, M.D. Perry, T.J. Phillips, T.C. Sangster, M.S. Singh, M.A. Stoyer, M. Tabak, G.L. Tietbohl, M. Tsukamoto, K. Wharton, S.C. Wilks, Phys. Plasmas 5 (1998) 1966.http://link.aip.org/link/doi/10.1063/1.872867.
[18] S.C. Wilks, W.L. Kruer, M. Tabak, A.B. Langdon, Phys. Rev. Lett. 69 (1992) 1383.http://prl.aps.org/abstract/PRL/v69/i9/p1383_1.
[19] P. Hakel, R.C. Mancini, J.C. Gauthier, E. Minguez, J. Dubau, M. Cornille, Phys. Rev. E 69 (2004) 056405. http://pre.aps.org/abstract/PRE/v69/i5/e056405.
[20] P. Hakel, R.C. Mancini, J. Abdallah, M.E. Sherrill, H.L. Zhang, J. Phys. B 42 (2009) 085701. http://pre.aps.org/forward/PRE/v75/i2/e026401.
[21] Y. Inubushi, Y. Okano, H. Nishimura, H. Cai, H. Nagatomo, T. Kai, T. Kawamura, D. Batani, A. Morace, R. Redaelli, C. Fourment, J.J. Santos, G. Malka, A. Boscheron, O. Bonville, J. Grenier, Ph. Canal, B. Lacoste, C. Lepage, L. Marmande, E. Mazataud, A. Casner, M. Koenig, S. Fujioka, T. Nakamura, T. Johzaki, K. Mima, Phys. Rev. E 81 (2010) 036410. http://pre.aps.org/abstract/PRE/v81/i3/e036410.
[22] M.F. Gu, Astrophys. J. 590 (2003) 1131. http://iopscience.iop.org/0004-637X/590/2/1131/.
[23] J. Myatt, W. Theobald, J.A. Delettrez, C. Stoeckl, M. Storm, T.C. Sangster, A.V. Maximov, R.W. Short, Phys. Plasmas 14 (2007) 056301. http://pop.aip.org/resource/1/phpaen/v14/i5/p056301_s1.

[24] I. Paterson, R.J. Clarke, N.C. Woolsey, G. Gregori, Meas. Sci. Technol. 19 (2008). http://iopscience.iop.org/0957-0233/19/9/095301/ 095301;
J. Howe, D.M. Chambers, C. Courtois, E. Förster, C.D. Gregory, I.M. Hall, O. Renner, I. Uschmann, N.C. Woolsey, Rev. Sci. Instrum. 77 (2006) 036105. http://link.aip.org/link/RSINAK/v77/i3/p036105/s1.
[25] http://physics.nist.gov/PhysRefData/ASD/lines_form.html.
[26] R.G. Evans, E.L. Clark, R.T. Eagleton, A.M. Dunne, R.D. Edwards, W.J. Garbett, T.J. Goldsack, S. James, C.C. Smith, B.R. Thomas, R. Clarke, D.J. Neely, S.J. Rose, Appl. Phys. Lett. 86 (2005) 191505. http://link.aip.org/link/doi/10.1063/1.1920422.
[27] P.M. Nilson, W. Theobald, J.F. Myatt, C. Stoeck, M. Storm, J.D. Zuege, R. Betti, D.D. Meyerhofer, T.C. Sangster, Phys. Rev. E 79 (2009) 016406. http://pre.aps.org/pdf/PRE/v79/i1/e016406.